



**HAL**  
open science

## Autoclave Sterilization of PEDOT:PSS Electrophysiology Devices

Ilke Uguz, Mehran Ganji, Adel Hama, Atsunori Tanaka, Sahika M Inal,  
Ahmed A Youssef, Roisin M Owens, Pascale P Quilichini, Antoine Ghestem,  
Christophe Bernard, et al.

► **To cite this version:**

Ilke Uguz, Mehran Ganji, Adel Hama, Atsunori Tanaka, Sahika M Inal, et al.. Autoclave Sterilization of PEDOT:PSS Electrophysiology Devices. *Advanced Healthcare Materials*, 2016, 5, pp.3094 - 3098. 10.1002/adhm.201600870 . hal-03796152

**HAL Id: hal-03796152**

**<https://amu.hal.science/hal-03796152>**

Submitted on 4 Oct 2022

**HAL** is a multi-disciplinary open access archive for the deposit and dissemination of scientific research documents, whether they are published or not. The documents may come from teaching and research institutions in France or abroad, or from public or private research centers.

L'archive ouverte pluridisciplinaire **HAL**, est destinée au dépôt et à la diffusion de documents scientifiques de niveau recherche, publiés ou non, émanant des établissements d'enseignement et de recherche français ou étrangers, des laboratoires publics ou privés.

# Autoclave Sterilization of PEDOT:PSS Electrophysiology Devices

*Ilke Uguz, Mehran Ganji, Adel Hama, Atsunori Tanaka, Sahika Inal, Ahmed Youssef, Roisin M. Owens, Pascale P. Quilichini, Antoine Ghestem, Christophe Bernard, Shadi A. Dayeh,\* and George G. Malliaras\**

Autoclaving, the most widely available sterilization method, is applied to poly(3,4-ethylenedioxythiophene) doped with polystyrene sulfonate (PEDOT:PSS) electrophysiology devices. The process does not harm morphology or electrical properties, while it effectively kills *E. coli* intentionally cultured on the devices. This finding paves the way to widespread introduction of PEDOT:PSS electrophysiology devices to the clinic.

I. Uguz, A. Hama, Dr. S. Inal, Prof. R. M. Owens,  
Prof. G. G. Malliaras

Department of Bioelectronics  
Ecole Nationale Supérieure des Mines  
CMP-EMSE, MOC  
13541 Gardanne, France  
E-mail: malliaras@emse.fr

M. Ganji, A. Tanaka, A. Youssef, Prof. S. A. Dayeh  
Department of Electrical and Computer Engineering  
Jacobs School of Engineering  
University of California, San Diego  
9500 Gilman Drive, La Jolla, CA 92093-0407, USA E-mail: sdayeh@ucsd.edu

Dr. P. P. Quilichini, A. Ghestem, Dr. C. Bernard  
Inserm U1106  
Institut de Neurosciences des Systèmes  
Aix Marseille University  
13005 Marseille, France

*Received: August 4, 2016*

**DOI: 10.1002/adhm.201600870**

The biological applications of organic electronic materials are currently attracting a great deal of interest [1-3]. One key thematic area encompasses the development of new devices for electrophysiology—devices that interface with cells by means of electrical recording and stimulation. Historically, interest in organics stems from their soft nature, which decreases the mechanical properties mismatch with tissue [4]. Another property that makes organics attractive to electrophysiology is their mixed electronic/ionic conductivity [5]. Indeed, organic coatings are shown to decrease the

**Table 1.** Results of the autoclave sterilization assay.  $N = 3$  solution samples taken from each array.

	<i>E. coli</i> exposure	Sterilization	OD at 600 nm	Sterile?
Reference 1		+	$0.05 \pm 0.01$	Yes
Reference 2	+		$1.68 \pm 0.05$	No
Array 1			$0.12 \pm 0.01$	No
Array 2		+	$0.05 \pm 0.01$	Yes
Array 3	+	+	$0.05 \pm 0.01$	Yes

electrochemical impedance at the biotic/abiotic interface and lead to better recordings and more efficient stimulation compared to traditional metal electrodes [6]. In addition to making better electrodes, mixed conductivity is leveraged to design novel devices with state-of-the-art properties. One such example is the organic electrochemical transistor (OECT), a device that uses an organic film as the transistor channel [7]. When used in vivo, ions from the cerebrospinal fluid, set in motion by neural firing, penetrate into the volume of the film and change its doping level. As a result of this volumetric response, OECTs act as efficient signal amplifiers and are being used to record brain activity with unprecedented signal-to-noise ratio [8].

The prototypical material used in organic-based electrophysiology devices is the conducting polymer poly(3,4-ethylenedioxythiophene) doped with polystyrene sulfonate (PEDOT:PSS). It is commercially available as an aqueous dispersion, and can be easily processed into films that are biocompatible and show high hole and ion conductivity [9]. PEDOT:PSS electrodes and OECTs are also used in in vitro diagnostics to monitor the health of cultures and tissue slices [10], and have been integrated with both rigid and flexible substrates to yield devices that interface with electrically active tissues in animal models [11,12]. Deposited on thin films of parylene, they make arrays that conform

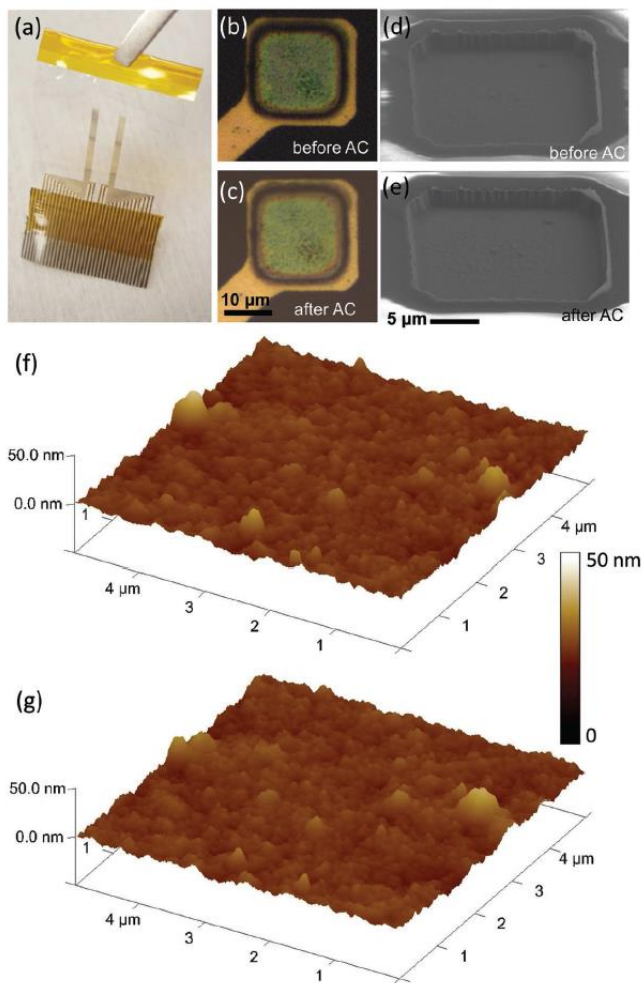


**Figure 1.** a) Picture of test geometry with two arrays, each containing 15 PEDOT:PSS microelectrodes. Optical microscopy images of the same microelectrode b) before and c) after autoclave. 45° angle view SEM images of the same microelectrode d) before and e) after autoclave. AFM topography images on a  $5 \times 5 \mu\text{m}^2$  area at the same location of PEDOT:PSS f) before and g) after autoclave.

well to the surface of the brain and yield stable, high signal-to-noise ratio cortical recordings in animal models as well as in humans [13]. Finally, PEDOT:PSS has been used in the fabrication of OECTs with record-high transconductance, used for electrophysiological recordings in animal models and in humans [8,14,15]. These efforts generate a great deal of potential for the realization of high-quality neural interfaces using organic materials. Such interfaces can be used to understand the brain, treat neurological diseases including epilepsy and Parkinson's, and yield stable brain/computer interfaces.

In order to transition these technologies to the clinic, effective sterilization that renders the devices free of pathogenic agents needs to be demonstrated. Several methods exist for the sterilization of medical devices, relying on heat, chemicals, or radiation to destroy potential pathogens. Among these, autoclaving is the most frequently used. The device to be sterilized is placed in a chamber and exposed to high pressure steam typically at a temperature of 121 °C for several minutes. The simplicity of the procedure and low cost of the equipment make this method widely available among biology laboratories and clinics worldwide. Unfortunately, however, autoclaving is not suitable for heat and

moisture-sensitive materials, which, a priori precludes its use with the vast majority of organic electronic devices. Indeed, few examples of organic-based devices can survive such a process, due to failure modes that include intrinsic materials degradation, morphological/structural changes, or mechanical damage due to thermal expansion [16]. It is worth noting that the first (and only so far) [13] clinical application of PEDOT:PSS relied on ethylene oxide sterilization, a method that is used for sterilization of disposable plasticware in bulk, and not directly available in most hospitals. A successful use of autoclaving would constitute an important step toward transitioning PEDOT:PSS devices from the lab to the clinic.

In this Communication, we show that sterilization of PEDOT:PSS electrophysiology devices can be performed using an autoclave. In a parallel study, conducted simultaneously in two laboratories in Gardanne (France) and in San Diego (California), we fabricated, sterilized, and tested PEDOT:PSS microelectrode and transistor arrays. We find that autoclaving is a viable sterilization method, leaving morphology unaltered and causing only minor changes in

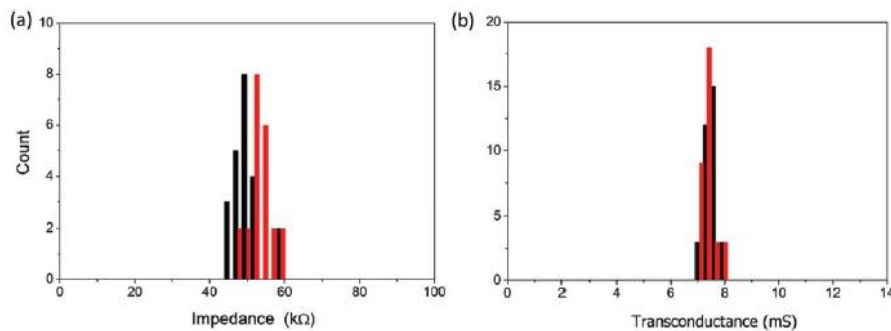


**Figure 2.** a) Histogram showing the distribution in electrode impedance at 1 kHz before (black) and after (red) sterilization. b) Histogram showing the distribution in OECT transconductance before (black) and after (red) sterilization.

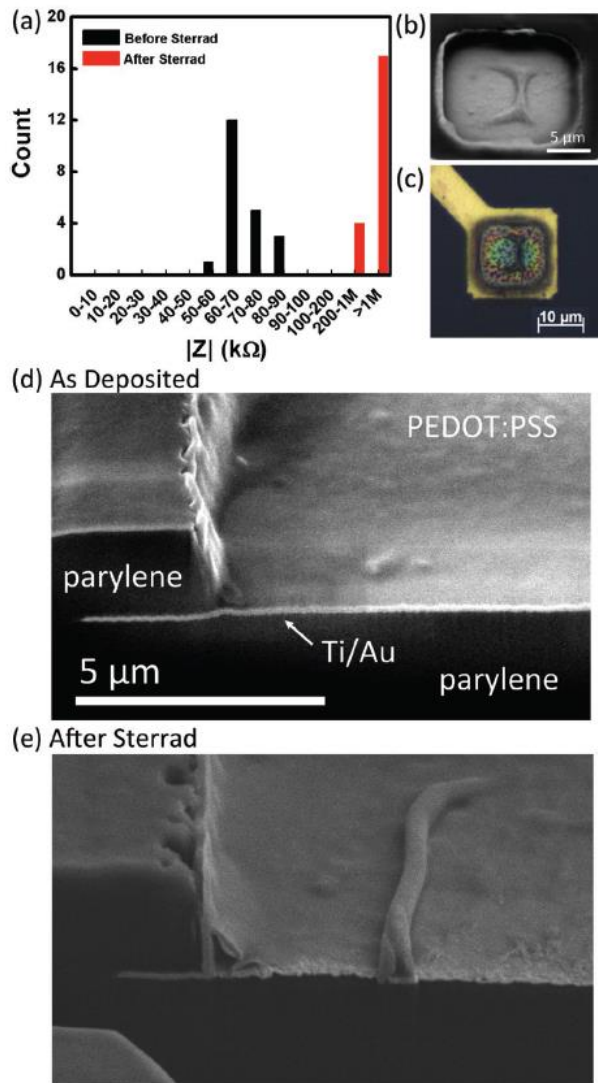


**Figure 3.** a) Impedance histogram at 1 kHz showing mostly open circuit devices after Sterrad sterilization. b) SEM image and c) optical image of a typical PEDOT:PSS microelectrode after Sterrad sterilization, showing clear delamination of the PEDOT:PSS microelectrode from Ti/Au near the edge and near the center after Sterrad sterilization. d,e) FIB cuts of the same electrode before and after sterilization.

electrical properties. These results pave the way for the widespread utilization of PEDOT:PSS electrophysiology devices in the clinic.

PEDOT:PSS microelectrode and OECT arrays were fabricated using lithography, as detailed in the Experimental Section. Each array consisted of a parylene substrate, Au pads/interconnects/electrodes, PEDOT:PSS islands, and a parylene layer

insulating the metal interconnects. In Gardanne, each array comprised 64 microelectrodes with sizes of  $10 \times 10$ ,  $20 \times 20$ , and  $40 \times 40 \mu\text{m}^2$ , or 13 OECTs with a channel length of  $5 \mu\text{m}$  and width of  $10 \mu\text{m}$ . The thickness of the PEDOT:PSS film was 220 nm. In San Diego, each array comprised 15 microelectrodes of  $15 \times 15 \mu\text{m}^2$  (Figure 1). The thickness of the PEDOT:PSS film was 280 nm. The arrays were autoclaved by exposure to steam at a temperature of  $121 \text{ }^\circ\text{C}$  for 20 min. We evaluated the efficacy of the sterilization process by intentionally inoculating a portion of the arrays with *Escherichia coli* (*E. coli*, ATCC 25922) before sterilization, as described in the Experimental Section. Immediately after sterilization, all arrays were incubated in culture media. After 24 h, the optical density (OD) of the media at 600 nm (OD<sub>600</sub> is a common method for estimating the concentration of bacteria in media) was measured. We defined boundary conditions by measuring the OD of autoclaved media (reference 1–sterile) and of media containing bacteria (reference 2–non-sterile), respectively. The results are summarized in Table 1. Array 1 was neither exposed to *E. coli* nor sterilized. Media in which the array was incubated showed an OD above the baseline, consistent with the array being non-sterile. Array 2 was not exposed to *E. coli* but was sterilized, resulting into optically clear media, consistent with the array being sterile. Array 3 was exposed to *E. coli* but was subsequently sterilized. Media in which the array was incubated was also clear, consistent with the array being sterile. These results, therefore, show that autoclaving renders the arrays sterile.

We next investigated the influence of autoclave sterilization on the

morphological stability of the microelectrodes by optical microscopy, scanning electron microscopy (SEM), and atomic force microscopy (AFM). The overall structure of the arrays is shown in Figure 1a. Optical images of the same microelectrode before (Figure 1b) and after (Figure 1c) autoclaving showed no evident morphological changes (the same holds for the whole device—no visible change was observed after sterilization). Similarly, SEM images on the same PEDOT:PSS microelectrode before (Figure 1d) and after (Figure 1e) autoclaving showed no evident delamination, cuts, or other observable morphological changes. To look further at the surface topography of the PEDOT:PSS at a higher resolution, we conducted AFM topography before (Figure 1f) and after (Figure 1g) autoclaving on the same  $5 \times 5 \mu\text{m}^2$  PEDOT:PSS location. The AFM images showed that the PEDOT:PSS morphology is generally conserved with a root mean square surface roughness of 3.41 nm before and 3.47 nm after autoclave.

For the electrodes, we measured the electrochemical impedance spectra as described in the Experimental Section. Impedance at 1 kHz is used as the benchmark for the characterization of neural electrodes, as this frequency corresponds to spiking activity<sup>[17]</sup>. Figure 2a shows a histogram of impedance values before and after sterilization, for electrodes with an area of  $10 \times 10 \mu\text{m}^2$  made and measured in Gardanne. The data show that the distribution moves slightly to higher values, with the average value changing from  $49.7 \pm 3.6 \text{ k}\Omega$  before sterilization to  $53.2 \pm 3.4 \text{ k}\Omega$  after. Similar results were obtained in San Diego, where average impedance values at 1 kHz changed from

$57.7 \pm 7.2 \text{ k}\Omega$  before sterilization to  $58.7 \pm 7.3 \text{ k}\Omega$  after sterilization.

For the OECTs, we measured the transfer curves as described in the Experimental Section and extracted transconductance. The transconductance is the key parameter that determines the performance of OECTs in electrophysiology, as it relates to signal amplification<sup>[18]</sup>. Figure 2b shows a histogram of transconductance values before and after sterilization, for devices made and measured in Gardanne. As with impedance, the change of the transconductance was very little after sterilization, from  $7.4 \pm 0.2$  to  $7.3 \pm 0.2 \text{ mS}$ . Furthermore, the resistance of the OECT channels was found to decrease by 4% after sterilization, indicating that materials degradation, changes in mobility/doping due to changes in microstructure, and/or delamination from contacts (though not detectable in Figure 1) might be underlying the changes in impedance and transconductance. These changes are, however, small, and the devices remain functional after autoclave sterilization.

The observed stability of the PEDOT:PSS electrophysiology devices to autoclaving can be attributed partly to the intrinsic thermal stability of their components and partly to the use of a cross-linker. Indeed, the devices are already baked during fabrication at  $140 \text{ }^\circ\text{C}$  for 1 h in ambient conditions, a temperature that all components of the device can sustain. Moreover, the cross-linker 3-glycidoxypropyltrimethoxysilane (GOPS) renders the PEDOT:PSS film insoluble to water. Devices made without GOPS do not survive autoclave sterilization, as the PEDOT:PSS film falls apart. It should be

noted that sterilization by autoclave does not seem to change the mechanical properties of parylene in a significant fashion (Figure S1, Supporting Information) and sterilized devices conform well to a 1:1 model of a rat brain (Figure S2, Supporting Information) and show the ability to record brain activity (Figure S3, Supporting Information).

While autoclaving showed no significant influence in the morphology and electrical characteristics of PEDOT:PSS devices, this is not a general case for all sterilization methods. As an example to the contrary we show results from chemical sterilization using the Sterrad system. This system destroys pathogens through exposure to H<sub>2</sub>O<sub>2</sub> gas plasma. Since the process does not typically exceed 50 °C, this method is particularly well-suited to heat and moisture-sensitive devices. However, Sterrad sterilization imparted extensive damage to PEDOT:PSS microelectrodes. As shown in Figure 3a, it resulted in nonfunctional devices, manifested by large impedance values. SEM and optical images in Figure 3b,c, respectively, depict severe morphological changes in the PEDOT:PSS film. By utilizing focused-ion beam (FIB) to section a PEDOT:PSS microelectrode before and after Sterrad sterilization (Figure 3d,e), we observed clear delamination of the PEDOT:PSS from the Ti/ Au metal lead at the center of the microelectrode and from the parylene at the edge of the microelectrode after the Sterrad process. The reason for this delamination is currently not clear. One possibility is that exposure to peroxide plasma causes extensive cross-linking of the PEDOT:PSS film, causing it to shrink and delaminate. Regardless of the

exact mechanism of failure, the negative result points to the fact that for each sterilization method, a systematic study needs to be undertaken to ensure suitability to a particular device.

In conclusion, we investigated the impact of sterilization methods on PEDOT:PSS microelectrodes and electrochemical transistors integrated on thin parylene supports. We show that devices inoculated with *E. coli* are effectively sterilized using autoclaving. The process does not alter appreciably the morphology of PEDOT:PSS films, while the electrical characteristics of microelectrodes and transistors show only minor degradation after exposure to steam. Sterrad sterilization, in contrast, causes large morphological changes in the PEDOT:PSS films and results in non-functional devices. The results show that autoclaving, which is readily available in most biological laboratories, is a viable sterilization method for PEDOT:PSS electrophysiology devices. This finding represents a significant step toward the widespread introduction of these devices to the clinic.

## Experimental Section

**Fabrication:** The fabrication of PEDOT:PSS-based electrodes and OECTs followed previously published processes<sup>[10]</sup>. In Gardanne, glass slides with dimensions of 7.62 × 2.54 cm<sup>2</sup> for OECTs and 4 × 4 cm<sup>2</sup> for electrodes, were cleaned by sonication in soap/water mixture and then in acetone/IPA mixture for 30 min. They were coated with 2 μm of parylene-C using an SCS Labcoater 2. For patterning

Au interconnects, S1813 (Shipley) photoresist was spin-coated on the glass slide, exposed to UV light using a SUSS MJB4 contact aligner, and developed using MF-26 developer. A thin (10 nm) Cr adhesion layer, followed by an Au film (100 nm) was deposited (Alliance Concept EVA450) and patterned using lift-off in acetone. A 1.8  $\mu\text{m}$  of parylene-C was deposited, acting as the insulation layer, and an additional, sacrificial layer of parylene-C (2  $\mu\text{m}$ ) was deposited, with a layer of soap in between. A 3.5  $\mu\text{m}$  of photoresist, AZ9260, was then patterned and etched using oxygen plasma with an Oxford 80 plus. Aqueous dispersion of PEDOT:PSS (PH 1000 from H.C. Stark) was mixed with ethylene glycol (EG, 5 vol%), dodecyl benzene sulfonic acid (DBSA, 0.2 vol%), and 3-glycidoxypropyltrimethoxysilane (GOPS, 1 wt %). The dispersion was spun-cast at 650 rpm for 30 s and the resulting film was patterned by peel-off of the top parylene-C film. The arrays were subsequently baked at 140  $^{\circ}\text{C}$  for 1 h and were immersed in deionized (DI) water to remove any excess low molecular weight compounds. In San Diego, glass slides ( $3 \times 3.5 \text{ cm}^2$ ) were used as substrate carriers for a thin parylene-C layer. The glass wafers were rinsed with acetone/IPA/water/IPA, sonicated for 5 min in IPA, and then rinsed again with acetone/IPA/water/IPA. Anti-adhesion film (Micro 90) was spin-coated at 650 rpm on the glass wafer to facilitate peeling-off the array at final step. A first parylene-C layer ( $\approx 3 \mu\text{m}$ ) was deposited using PDS 2010 Parylene Coater system. Ti/Au (10 nm/100 nm) metal leads were defined using a lift-off process in acetone with a NR9-3000 negative resist for photolithography and a Temescal BJD 1800 electron beam evaporator for the 10 nm Ti adhesion layer

and 100 nm Au layer deposition. Prior to the second parylene-C deposition, an adhesion promoter (Silane A-174:H<sub>2</sub>O:IPA with 1:200:200) was applied. The encapsulating parylene-C layer ( $\approx 2.2 \mu\text{m}$ ) was then deposited and coated with another Micro 90 anti-adhesion film. A third layer parylene-C was then deposited, followed by the spin-coating of a thick 2010 SU-8 layer, which was exposed using a Karl Suss MA6 Mask Aligner and developed with SU-8 developer. Oxygen plasma (Oxford Plasmalab 80 RIE) was used to etch and define the openings for the subsequent PEDOT:PSS layer. Aqueous dispersion of PEDOT:PSS (PH 1000 from Clevios) was mixed with EG (5 vol%), DBSA (0.2 vol%), and GOPS (1 wt %). The solution was spin-coated at 650 rpm for 30 s and pre-baked at 95  $^{\circ}\text{C}$  for 1 min. The third parylene-C layer was peeled-off to pattern the PEDOT:PSS on top of the electrode sites. Finally, the arrays were cured at 140  $^{\circ}\text{C}$  for 1 h and immersed in DI water to remove any excessive components from the PEDOT:PSS.

**Characterization:** FEI SFEG UHR SEM was used to take high-resolution images at 10 kV with 4702 $\times$  magnification. For sample preparation, a thin layer of the Ti (15 nm) has been deposited at back of the array in order to reduce the charging effects during the imaging. A Veeco Scanning Probe Microscope was used to take AFM images in tapping mode. Electrochemical impedance spectroscopy (EIS) was performed using a GAMRY interface 1000E in phosphate buffer saline (PBS) solution, using three-electrode configuration, i.e., Ag/AgCl electrode as a reference, platinum as a counter, and PEDOT:PSS a working electrode. Sinusoidal signals with 10 mV rms AC voltage and zero DC voltage were



applied and the frequency was swept from 100 kHz to 1 Hz to achieve complete capacitive and faradaic domains. In Gardanne, impedance spectra were measured with an Autolab PGSTAT equipped with an FRA module. The measurements were carried out in PBS using a three electrode configuration using the same parameters as in San Diego. The OECTs were characterized in PBS with an Ag/AgCl gate electrode, using a Keithley 2612A dual SourceMeter and customized LabVIEW software. The transconductance reported here was measured at a drain voltage of  $-0.6$  V and a gate voltage of 0 V.

**Sterilization:** In Gardanne, sterilization of the devices was achieved using a Tuttnauer Model 3150EL autoclave. The samples were placed into autoclave pouches and sealed prior to exposure to steam. A 20 min treatment with saturated steam at 121 °C was followed by a 15 min evaporative drying step. Some of the devices were inoculated with 200  $\mu$ L pre-culture (*E. coli* ATCC 25922), sterilized by autoclave and placed in pre-sterilized flasks that contained Luria-Bertani media (Sigma). The arrays were incubated for 24 h at 37 °C. The optical density of the resultant microbial population was measured at a wavelength of 600 nm using a TECAN M1000 spectrophotometer. In San Diego, autoclave sterilization was performed using a SUN series autoclave (Class B). Arrays were directly exposed to water vapor at 121 °C for 20 min. Sterrad sterilization was performed by exposing arrays to hydrogen peroxide vapor at 50 °C for 47 min, at UCSD's Thornton Hospital, while the arrays were kept in appropriate sterilization pouches.

## Supporting Information

Supporting Information is available from the Wiley Online Library or from the author.

## Acknowledgements

I.U. and M.G. contributed equally to this work. The authors would like to acknowledge support from the Fondation pour la Recherche Médicale under Grant Agreement No.DBS20131128446, the Region PACA, and Microvitae Technologies. The authors would also like to acknowledge support from the Center for Brain Activity Mapping at UC San Diego under Grant No. 2014-018CBAM. The authors thank Georges Hadziioannou (Bordeaux) and Christopher Ober (Cornell) for fruitful discussions on the stability of PEDOT:PSS, and Eloise Bihar and Magali Ferro for help with the measurements of mechanical properties.

## References

- [1] M. Berggren, A. Richter-Dahlfors, *Adv. Mater.* **2007**, *19*, 3201.
- [2] J. Rivnay, R. M. Owens, G. G. Malliaras, *Chem. Mater.* **2014**, *26*, 679.
- [3] C. Liao, M. Zhang, M. Y. Yao, T. Hua, L. Li, F. Yan, *Adv. Mater.* **2015**, *27*, 7493.
- [4] D.-H. Kim, S. Richardson-Burns, L. Povlich, M. R. Abidian, S. Spanninga, J. Hendricks, D. C. Martin, in *Indwelling Neural Implants. Strategies for Contending with the In Vivo Environment*. (Ed: W. M. Reichert), CRC Press, Boca Raton, FL **2008**, pp. 165-207.
- [5] J. M. Leger, *Adv. Mater.* **2008**, *20*, 837.

- [6] D. C. Martin, G. G. Malliaras, *ChemElectroChem* **2016**, *3*, 686.
- [7] H. S. White, G. P. Kittlesen, M. S. Wrighton, *J. Am. Chem. Soc.* **1984**, *106*, 5375.
- [8] D. Khodagholy, T. Doublet, P. Quilichini, M. Gurfinkel, P. Leleux, A. Ghestem, E. Ismailova, T. Hervé, S. Sanaur, C. Bernard, G. Malliaras, *Nat. Commun.* **2013**, *4*, 1575.
- [9] J. Rivnay, S. Inal, B. A. Collins, M. Sessolo, E. Stavrinidou, X. Strakosas, C. Tassone, D. M. DeLongchamp, G. G. Malliaras, *Nat. Commun.* **2016**, *7*, 11287.
- [10] M. Sessolo, D. Khodagholy, J. Rivnay, F. Maddalena, M. Gleyzes, E. Steidl, B. Buisson, G. G. Malliaras, *Adv. Mater.* **2013**, *25*, 2135.
- [11] M. D. Johnson, R. K. Franklin, M. D. Gibson, R. B. Brown, D. R. Kipke, *J. Neurosci. Methods* **2008**, *174*, 62.
- [12] D. Khodagholy, T. Doublet, M. Gurfinkel, P. Quilichini, E. Ismailova, P. Leleux, T. Herve, S. Sanaur, C. Bernard, G. G. Malliaras, *Adv. Mater.* **2011**, *23*, H268.
- [13] D. Khodagholy, J. N. Gelinas, T. Thesen, W. Doyle, O. Devinsky, G. Malliaras, G. Buzsaki, *Nat. Neurosci.* **2015**, *18*, 310.
- [14] A. Campana, T. Cramer, D. T. Simon, M. Berggren, F. Biscarini, *Adv. Mater.* **2014**, *26*, 3874.
- [15] J. Rivnay, P. Leleux, M. Ferro, M. Sessolo, A. Williamson, D. A. Koutsouras, D. Khodagholy, M. Ramuz, X. Strakosas, R. M. Owens, C. Benar, J.-M. Badier, C. Bernard, G. G. Malliaras, *Sci. Adv.* **2015**, *1*, e1400251.
- [16] K. Kuribara, H. Wang, N. Uchiyama, K. Fukuda, T. Yokota, U. Zschieschang, C. Jaye, D. Fischer, H. Klauk, T. Yamamoto, K. Takimiya, M. Ikeda, H. Kuwabara, T. Sekitani, Y.-L. Loo, T. Someya, *Nat. Commun.* **2012**, *3*, 723.
- [17] G. Buzsáki, C. A. Anastassiou, C. Koch, *Nat. Rev. Neurosci.* **2012**, *13*, 407.
- [18] J. Rivnay, P. Leleux, M. Sessolo, D. Khodagholy, T. Herve, M. Fiochi, G. G. Malliaras, *Adv. Mater.* **2013**, *25*, 7010.